Eur. Phys. J. B **44**, 381–393 (2005)
DOI: 10.1140/epjb/e2005-00137-0

THE EUROPEAN PHYSICAL JOURNAL B

Interfacial properties in solid-stabilized emulsions

S. Arditty[1], V. Schmitt[1,a], F. Lequeux[2], and F. Leal-Calderon[3]

[1] Centre de Recherche Paul Pascal, CNRS, Avenue Schweitzer, 33600 Pessac, France
[2] Laboratoire de Physicochimie Macromoléculaire, ESPCI, 10 rue Vauquelin, 75231 Paris Cedex 05, France
[3] Laboratoire des Milieux Dispersés Alimentaires, ISTAB, Avenue des facultés, 33405 Talence, France

Received 15 December 2004
Published online 28 April 2005 –

Abstract. We prepared concentrated monodisperse oil-in-water emulsions stabilized by solid particles. The osmotic resistance, Π, of the emulsions was measured for different oil volume fractions above the random close packing ($\phi^* \approx 64\%$). The dimensionless osmotic resistance, $\Pi/(\gamma/R)$ (γ being the interfacial tension and R being the undeformed drop radius), was always substantially higher than the corresponding values obtained for surfactant-stabilized emulsions. It can be concluded that droplet deformation in solid-stabilized emulsions is not controlled by the capillary pressure, γ/R, of the non-deformed droplets but rather by σ_0/R, σ_0 being a parameter characterizing the rigidity of the droplets surfaces. The data can be interpreted considering that the interfacial layers are elastic at small deformations and exhibit plasticity at intermediate deformations. σ_0 corresponds to the surface yield stress, i.e. the transition between elastic and plastic regimes. We discuss the origin of the surface behavior considering the strong lateral interactions that exist between the adsorbed solid particles. We propose an independent measurement of σ_0 based on the critical bulk stress that produces droplet fragmentation in dilute emulsions submitted to shear. Finally, the bulk shear elastic modulus was measured as a function of ϕ and confirms many of the features revealed by the osmotic resistance.

PACS. 82.70.-y Disperse systems; complex fluids – 82.70.Kj Emulsions and suspensions – 68.15.+e Liquid thin films

Introduction

Emulsions are metastable systems normally obtained in the presence of different surface-active species like surfactant molecules, amphiphilic polymers or proteins. It is now well established that solid particles of colloidal size may also be employed to kinetically stabilize emulsions [1–3]. A growing interest is being devoted to the so-called Pickering or solid-stabilized emulsions [4], as they may advantageously replace conventional emulsions containing organic surfactants. The solid particles are irreversibly anchored at the oil-water interface and develop strong lateral interactions [4]. In Pickering emulsions, the stabilizing film between the droplets is composed of very rigid layers that provide a mechanical barrier against coalescence.

Emulsions are dispersions of deformable droplets; hence, different interfacial configurations can be achieved as a function of the oil volume fraction, ϕ. Although frequently comprising Newtonian fluids, emulsions become remarkably rigid and resemble an elastic solid at high droplet volume fraction. As pointed by Princen [5] and Mason et al. [6–8], the considerable elasticity of the concentrated emulsions exists because the repulsive droplets have been compressed by an external osmotic pressure, Π. Two droplets forced together will begin to deform before their interfaces actually touch, due to the intrinsic repulsive interactions between them. Thus, emulsions minimize their total free energy by reducing the repulsion (which may have different origins) at the expense of creating some additional surface area by deforming the droplet interfaces. The necessary work to deform the droplets is done through the application (by any means) of an external osmotic pressure, Π, and the excess surface area of the droplets determines the equilibrium elastic energy stored at a given osmotic pressure. Additional excess surface area created by a perturbative shear deformation, determines the elastic shear modulus, $G(\phi)$. Although Π and G represent fundamentally different properties, they both depend on the degree of droplet deformation and therefore on ϕ.

The first quantitative study on the elastic properties of monodisperse emulsions was performed by Mason et al. [6]. They investigated silicon oil-in-water emulsions stabilized by sodium dodecyl sulfate (SDS). The osmotic pressure and the shear modulus were of the same order of magnitude and both were found to increase by nearly four decades as ϕ increases from 0.5 to about 0.9. They both exhibit a universal dependence on the effective oil

[a] e-mail: schmitt@crpp-bordeaux.cnrs.fr

volume fraction, when scaled with the Laplace pressure of the non-deformed droplets. The scaling with γ/R (γ being the interfacial tension and R being the drop radius) confirms that the elasticity of compressed monodisperse emulsions depends only on the packing geometry of the droplets.

The aim of the experiments reported in the present paper is to measure the bulk properties of solid-stabilized concentrated emulsions and to deduce some characteristic properties of the interfacial layers covering the droplets. For that purpose, concentrated monodisperse oil-in-water emulsions stabilized by solid particles were fabricated following a limited coalescence process [3,9–11]. The osmotic resistance, Π, of the emulsions was measured for different oil volume fractions above the random close packing ϕ^*. Due to droplet deformation, the experimental curve $\Pi(\phi)$ reflects the mechanical properties of the layers formed by the solid particles at the oil-water interface. The dimensionless quantity, $\Pi/(\gamma/R)$, was always substantially higher than the corresponding values obtained for surfactant-stabilized emulsions. We demonstrate that droplet deformability in solid-stabilized emulsions is not controlled by γ/R but rather by σ_0/R, σ_0 being a parameter characterizing the rigidity of droplets surfaces. We propose a model that links the osmotic pressure and the interfacial energy. The droplet surfaces can be regarded as compact 2-D networks of solid particles with strong lateral attractive interactions. The osmotic pressure data can be interpreted considering that the surfaces are elastic at weak deformations and exhibit plasticity at intermediate deformations. σ_0 corresponds to the 2-D yield stress, i.e. the transition between elastic and plastic regimes. We justify the order of magnitude of σ_0 considering the main lateral interactions that exist between the adsorbed solid particles. Then, a second route to evaluate σ_0 is proposed: it consists of submitting dilute emulsions to simple shear and to measure the critical stress that produces droplet fragmentation.

1 Experimental section

1.1 Materials

Solid particles were prepared using an aqueous dispersion of monodisperse, spherical, hydrophilic precipitated silica purchased from Clariant (Klebosol 30R25). The average primary particle diameter is $d_p = 25$ nm, as deduced from light scattering measurements using a Malvern ZetaSizer HS 3000 instrument. The particle density is $\rho_p = 2.1\ \mathrm{g\,cm^{-3}}$. The surface of such particles was made partially hydrophobic by chemically grafting n-octyltriethoxysilane (hydrolysis-condensation reaction) to an estimated density of 5 chains $\mathrm{nm^{-2}}$, in order to favor adsorption at the oil-water interface. The particles were transferred from the synthesis media into pure water by dialysis. Particles were flocculated in the aqueous phase with a floc size of around 0.5 μm. The dispersions were sonicated before making the emulsions, which resulted in a significant reduction of the average floc size.

The oils used were polydimethylsiloxane (PDMS) of viscosity 350 mPa.s (Rhodorsil 47V350; density $\rho_o = 0.98\ \mathrm{g\,cm^{-3}}$), and dodecane (Puriss grade, Fluka; $\rho_o = 0.75\ \mathrm{g\,cm^{-3}}$). Water was passed through a Millipore purifier and had a resistivity of 18 MΩ.cm.

1.2 Methods

1.2.1 Emulsion preparation

The method employed to obtain solid-stabilized monodisperse emulsions is based on a limited coalescence process [9–11]. It consists of producing a large excess of oil-water interface compared to the amount that can be potentially covered by the solid particles. For this process to occur, the systems were always formulated in the presence of a very small amount of solid particles (approximately 200 mg to 500 mg for 100 g of dispersed phase). When the agitation is stopped, the partially unprotected droplets coalesce, thus reducing the total amount of oil-water interface. Since the particles are irreversibly adsorbed, the coalescence process stops as soon as the oil-water interface is sufficiently covered [9–11]. The resulting emulsions are stable over months and remarkably monodisperse. The final mean droplet diameter can be controlled by adjusting the amount of particles. Because the solid particles are totally and irreversibly adsorbed (no free particles in the continuous phase), the inverse average droplet diameter varies linearly with the amount of particles [10]:

$$\frac{1}{D} = \frac{s_f m_p}{6V_d} \tag{1}$$

where m_p is the mass of particles, V_d is the volume of dispersed phase, s_f is the specific surface area, i.e. the droplet surface covered per unit mass of silica. In the present study, oil-in-water (o/w) emulsions were produced using a jet homogenizer (Microfluidics M110S) with a pressure in the homogenizing chamber varying between 250 and 1600 bars. The important energy input enables the stabilization of emulsions with average diameter ranging from 1 μm to 25 μm. Figure 1 provides an example confirming the validity of relation (1). For the systems under study, we find $s_f = 24\ \mathrm{m^2\,g^{-1}}$ for both PDMS-in-water and dodecane-in-water emulsions. A densely packed layer of adsorbed particles (2-D compacity of 0.9) would provide a s_f value of $32\ \mathrm{m^2\,g^{-1}}$.

1.2.2 Droplet size measurements

The droplet size distributions of the emulsions were measured with a static light scattering apparatus (Mastersizer S, Malver Instruments) using Mie theory. Starting from the volume distribution, a little bit of algebra allows a straightforward calculation of the surface average diameter D defined as:

$$D = \left(\frac{\sum_i N_i D_i^3}{\sum_i N_i D_i^2} \right) \tag{2}$$

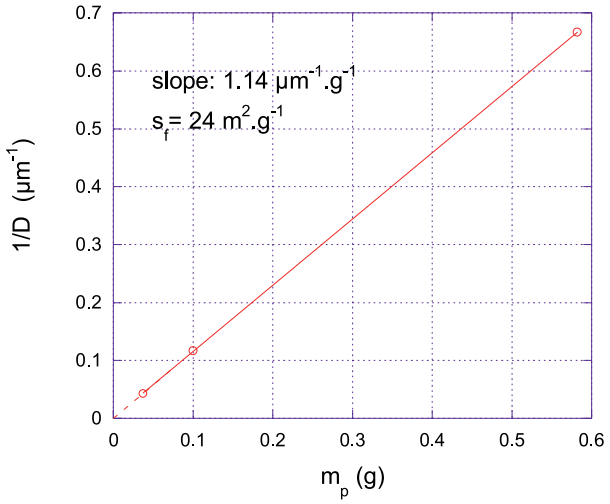

Fig. 1. Evolution of the inverse diameter as a function of the mass of solid particles for PDMS-in-water emulsions stabilized by hydrophobically modified silica particles.

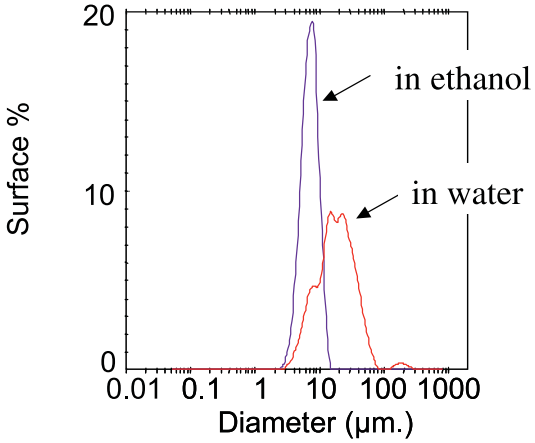

Fig. 2. Size distributions of PDMS droplets dispersed in water and in ethanol.

where N_i is the total number of droplets with diameter D_i. The emulsions were characterized in terms of their surface-averaged diameter D and polydispersity, P:

$$P = \frac{1}{\overline{D}} \frac{\sum_i N_i D_i^2 \left| \overline{D} - D_i \right|}{\sum_i N_i D_i^2}, \qquad (3)$$

where $\overline{D}$ is the median diameter for which the cumulative undersized volume fraction is equal to 50%.

The average droplet size provided by the granulometer was checked by observing the emulsions with a phase contrast optical microscope (Zeiss, Axiover, X 100). A difficulty arises from the fact that the emulsions were partially or totally flocculated in pure water. In Figure 2, we report a typical distribution obtained in pure water, reflecting the presence of agglomerates. This is why the emulsions were diluted with ethanol in the measuring cell. This solvent, combined with a gentle agitation, had the effect to disrupt almost all the flocs initially present in the emulsion. Figure 2 also contains the granulometric distribution obtained in ethanol for the same emulsion. The distribution is now monomodal and quite narrow, as could be expected from the observation of the individual droplets under the microscope. For the emulsions under study, the polydispersity was always smaller than 35%.

1.2.3 Interfacial tension measurements

The interfacial tension γ between oil and pure water was determined at equilibrium using a Wilhelmy balance ($T = 20$ °C). The obtained values were $\gamma = (30 \pm 2) \times 10^{-3}$ N m^{-1} for the PDMS/water interface and $\gamma = (50 \pm 2) \times 10^{-3}$ N m^{-1} for the dodecane/water interface.

1.2.4 Measurements of the elastic and dissipation moduli. Oscillatory rheology

When a small shear stress, τ, is applied to a solid, the resulting deformation, Γ, is proportional to τ, with $\tau = G\,\Gamma$, where G is the elastic shear modulus. For materials which do not store perfectly the energy, G can be generalized as the sum of two contributions. The in-phase contribution G' is linked to the stored energy while the $\pi/2$ out-of-phase contribution G'' is related to the dissipated energy. For complex systems, the relative contributions may be frequency-dependent.

Oscillatory rheological experiments were performed with a controlled-strain Rheometrics RFSII rheometer. A sinusoidal strain is applied at a given frequency and the response of the system (the time-dependent stress) is measured. As long as the oscillatory strain amplitude is low enough to be considered as a perturbation (linear regime), the resulting stress is also sinusoidal with an amplitude proportional to the strain. Above a certain value of the applied strain, the response of the material is no more sinusoidal. In this limit, the material begins to flow and the deformation is no more perturbative: G' and G'' become strain dependent and should only be considered as apparent.

The experiments were performed using a parallel plate geometry with a gap of 1 mm. Despite the fact that the applied stress is not constant over the whole sheared volume, this type of geometry was preferred in order to avoid problems related to confinement. The plate surfaces were made rough in order to avoid any slip at the walls. A solvent trap prevents water evaporation from the samples during the measurements.

1.2.5 Osmotic pressure measurements

In order to measure the evolution of the osmotic pressure, we centrifuged a known amount of dilute emulsion and then determined the droplet volume fraction ϕ_f at the top or the bottom of the centrifugation tube. Due to the presence of solid particles at the oil-water interface, the

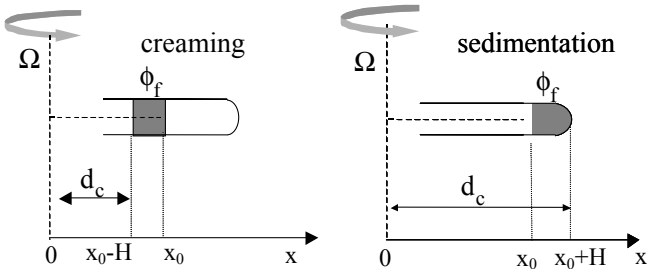

Fig. 3. Scheme of the centrifugation experiment. See text for details.

average density of the droplets, ρ_d, can be larger than that of the continuous phase:

$$\rho_d = \rho_o + \frac{6}{Ds_f}. \tag{4}$$

Thus, emulsions with small average droplet diameter tend to sediment, while those with large average diameters preferentially cream. After creaming or sedimenting, if the droplets occupy a distance much less than that of the centrifuge lever arm, the spatial gradient in the acceleration can be neglected, and the osmotic pressure can be determined (see Fig. 3):

$$\Pi = |\Delta\rho|\ \Omega^2\,\phi_f\,\left(d_c H \pm \frac{H^2}{2}\right) \tag{5}$$

where H is the final height of the cream/sediment, ϕ_f is the final oil volume fraction, $\Delta\rho = \rho_d - \rho_c$ is the density mismatch between oil and the continuous phase, d_c is the length of the lever arm and Ω is the rotation speed of the centrifuge. In the right hand term of equation (5), the operator + applies to creaming and – to sedimentation. This maximum osmotic pressure reflects the stress exerted by the droplet layers below (above) the top (bottom) of the cream (sediment). The centrifugation typically takes several hours until the equilibrium volume fraction is achieved. The centrifuge employed was Optima TLX Ultracentrifuge (Beckman) equipped with a swinging-bucket rotor, model TLS-55.

The volume fraction of the droplets at the top (bottom) was determined in the following way. A part of each emulsion sample was carefully collected from the top (bottom) of the concentrated cream (sediment) and left in a dry oven at 40 °C for approximately 10 hours. This time is sufficient for complete evaporation of the continuous phase. We verified that for the same period of time the volatility of the oil phase is negligible. Therefore, weighing the samples before and after the continuous phase evaporation provides a simple way to determine the droplet volume fraction.

Right after centrifugation, the samples were stored at room temperature for several days. Within this period of time, there was no visible swelling of the cream or sediment. The absence of swelling suggests that either compaction of the droplets is irreversible or decompression is extremely slow. The osmotic pressure is a force per unit surface capable of causing the expansion of the system. This is the case for the osmotic pressure of molecular solutions and of non aggregated colloidal dispersions. Since our emulsions do not expand after several days if the applied pressure is set to zero, we more likely measure an osmotic resistance which eventually arises from a plastic behavior. The origin of Π will be discussed in more detail in Section 3.1. For the sake of generality, hereafter, the parameter Π defined in equation (5) will be termed "osmotic resistance".

1.2.6 Shear experiments on single droplets

The aim of the following experiments is to measure the necessary stress that produces fragmentation of single droplets. Monodisperse PDMS-in-water emulsions were initially fabricated using the jet homogenizer. The resulting diameter is 8 μm in agreement with the 24 $m^2\,g^{-1}$ value obtained for s_f (same surface coverage as the previous emulsions). Dilute emulsions are submitted to a step in shear stress (non quasi-static conditions) in the gap of a stress-controlled rheometer (AR 1000, TA Instruments) equipped with a cone and plate geometry. To obtain rupturing at shear rates that were accessible to our rheometer (<1000 s^{-1}), it was necessary to transfer the solid-stabilized droplets in highly viscous solutions. Two different water-soluble polymers were adopted for that purpose: polyacrylic acid (PAA, provided by Fluka) with molecular mass $M_w \approx 500\,000$ g/mol and polyethylene glycol (PEG, provided by Fluka) with $M_w \approx 35\,000$ g/mol. Both polymers only act as thickening agents and have a negligible interfacial activity. The droplet volume fraction was $\phi = 1\%$ and the polymer concentrations in water (20 %w for PAA and 64 %w for PEG) were adjusted to obtain a viscosity of 60 Pa in the explored stress range: $0 < \tau < 6000$ Pa. The emulsions were then submitted to different steps in shear stress for a given time $t \geq 10$ s. After shearing cessation, the emulsions were observed under a microscope to determine whether fragmentation has occurred or not. Droplet fragmentation is revealed by a discrete jump of the droplets size before and after application of the stress.

2 Results

2.1 Osmotic resistance measurements

2.1.1 Influence of the aggregation state

As described above, the droplet size of the emulsions is reproducibly controlled by the compositional parameters (V_d, m_p) through equation (1). By changing the pressure in the jet homogenizer at constant composition, we could obtain emulsions with the same droplet size but different states of aggregation. Although the extent of flocculation was not easy to control, we noticed that increasing the amount of solid particles or decreasing the pressure in the homogenizing chamber (everything else being constant) preferentially led to strongly aggregated systems.

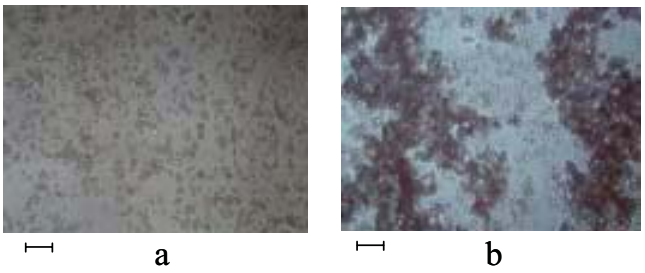

Fig. 4. Microscopic images of PDMS-in-water emulsions with average diameter $D \approx 9$ μm. Scale bar = 50 μm.

For example, the microscope images in Figure 4 correspond to PDMS-in-water emulsions fabricated at different pressures in the homogenizing chamber. The two emulsions possess approximately the same droplet diameter $D \approx 9$ μm, and are characterized by identical s_f values: $s_f = 24$ m^2 g^{-1} (deduced from $1/D$ versus m_p plots). However, the aggregation state is completely different from one system to the other: the emulsion in Figure 4a obtained at 1500 bars in the homogenizing chamber only contains small clusters and a large fraction of individual droplets, while that in Figure 4b fabricated at 250 bars essentially comprises large aggregates than span over the whole field of the microscope. The difference in the flocculation state can be evidenced by a simple creaming experiment. The same systems with initial droplet fraction $\phi_i = 14\%$ are stored at rest and we observe their macroscopic evolution as a function of time. After 24 hours, the emulsion with only small clusters forms a dense creamed layer with final volume fraction $\phi_f \approx 40-45\%$: droplets or cluster rearrangements occur quite easily in this weakly aggregated system leading to a rapid compaction under the effect of buoyancy. Instead, the emulsion containing large clusters undergoes only a weak compaction ($\phi_f \approx 20\%$) which suggests that the aggregated structure is not easily disrupted by the gravitational stress. Hence we have two emulsions with the same size, same coverage and different aggregation states at our disposal. The emulsions were centrifuged following the method described in the experimental section (Sect. 1.2.5) in order to obtain the Π versus ϕ curves. In the experimental conditions adopted here ($\Omega > 5000$ rpm), we could only explore the concentrated regime: $\phi > 70\%$. In Figure 5, we report the experimental data obtained for the two previously mentioned emulsions. It clearly appears that the aggregation state has a strong impact on the osmotic resistance: at any droplet fraction ϕ, the Π values are 3−5 times larger for the strongly aggregated system.

Another way of changing the aggregation state consists of modifying the composition of the continuous phase. A primary emulsion with diameter $D = 1.5$ μm was fabricated in pure water and was substantially aggregated. The continuous phase was extracted and replaced by pure ethanol. After gentle stirring, the daughter emulsion containing ethanol was almost totally re-dispersed. Figure 6 again illustrates the influence of the flocculation state on the osmotic resistance. The emulsion containing pure

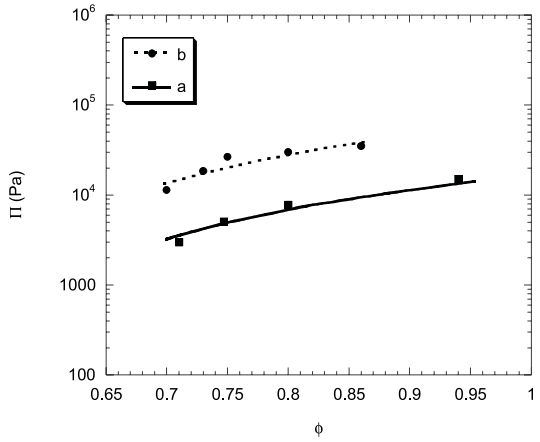

Fig. 5. Evolution of the osmotic resistance Π as a function of the droplet volume fraction ϕ for the emulsions shown in Figure 4. The lines are guides to the eyes.

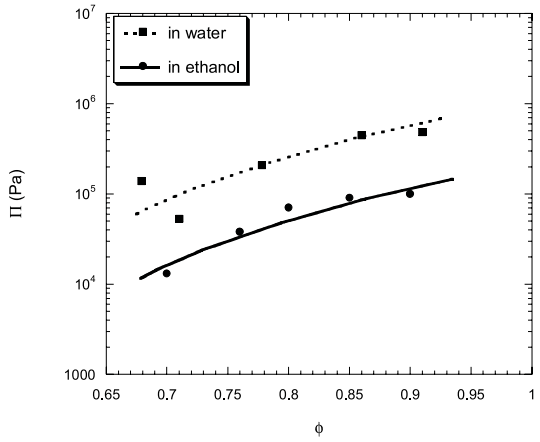

Fig. 6. Evolution of the osmotic resistance Π as a function of the droplet volume fraction ϕ for PDMS droplets with diameter $D = 1.5$ μm, dispersed in pure water and in pure ethanol. The lines are guides to the eyes.

ethanol is quite well dispersed and the osmotic resistance measured is 3−5 times smaller than the one obtained for the aggregated emulsion in pure water.

The examples given in Figures 5 and 6 were selected because they illustrate two limiting situations with respect to droplet aggregation. The same factor (3-5) was systematically found between the osmotic resistance of weakly and strongly flocculated systems, whatever the droplet size. Of course, intermediate situations can be found and lie within the two previous limits. In the following, we shall systematically specify the aggregation state of the emulsions based on observations of the samples under the microscope.

2.1.2 Influence of the droplet size

We performed a set of experiments in which we varied the average droplet size. The graph in Figure 7 shows the dependence of the normalized (by γ/R) osmotic resistance as a function of the oil (PDMS) volume fraction.

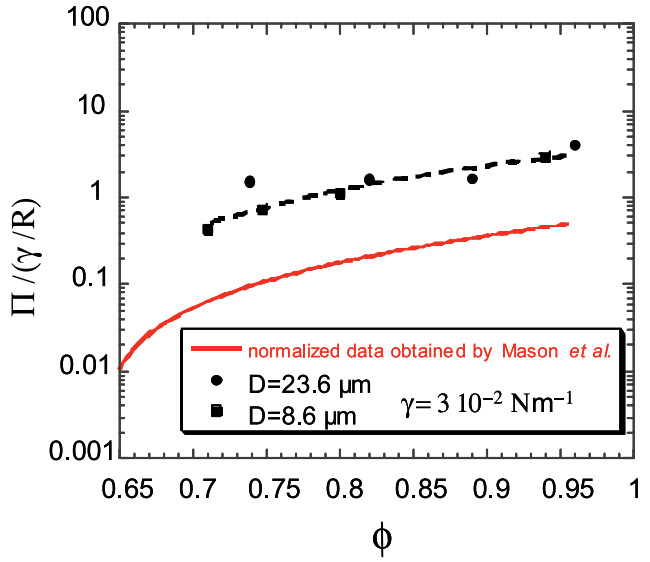

Fig. 7. Evolution of the osmotic resistance Π normalized by γ/R for weakly aggregated PDMS-in-water emulsions. The dashed line is a guide to the eyes. The solid line corresponds to the best fit of the normalized data obtained by Mason et al. [6].

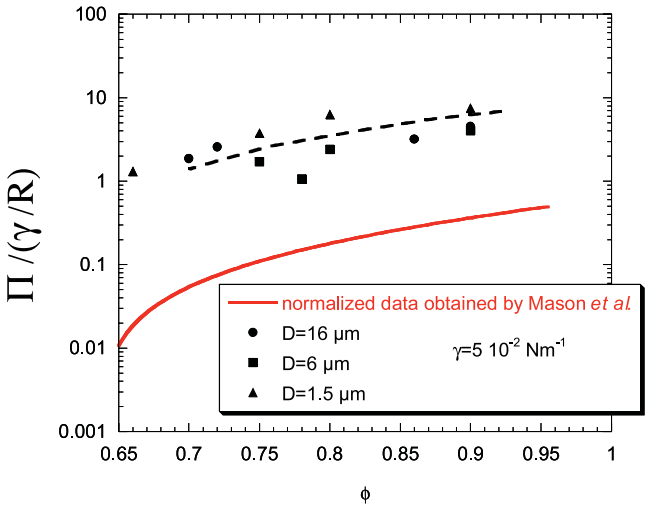

Fig. 9. Evolution of the osmotic resistance Π normalized by γ/R for strongly aggregated dodecane-in-water emulsions. The dashed line is a guide to the eyes. The solid line corresponds to the best fit of the normalized data obtained by Mason et al. [6].

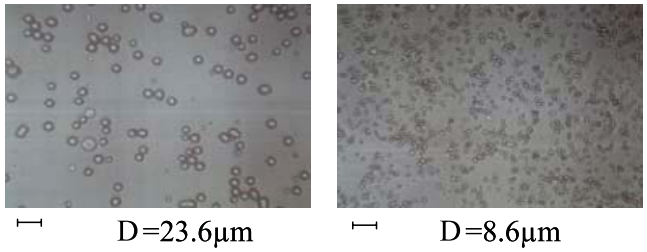

Fig. 8. Microscopic images of two weakly flocculated PDMS-in-water emulsions. Scale bar = 50 μm.

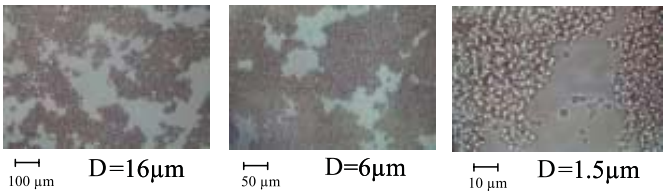

Fig. 10. Microscopic images of the three strongly flocculated dodecane-in-water emulsions used to obtain Figure 9.

The droplets were only weakly flocculated as can be deduced from the images of Figure 8. It is instructive to plot the data in $\Pi/(\gamma/R)$ versus ϕ coordinates: this type of plot provides a possibility to compare the results with the literature data excluding the effects of droplet size and interfacial tension. In principle, it is also necessary to transform the oil volume fraction in effective oil volume fraction, in order to take into account the repulsive interactions between the droplets. Actually, as pointed by Mason et al. [6], the effective oil volume fraction takes into account the thin films which exist between the deformed droplets. The effective oil volume fraction, ϕ_{eff} can be calculated as:

$$\phi_{eff} = \phi \left[1 + \frac{h}{D}\right]^3 \qquad (6)$$

where h is the thickness of the films between the droplets at volume fraction ϕ. It is reasonable to suppose that the film thickness, h, is of the same order than the particle diameter (25 nm). For all the emulsions that were probed, the droplet diameter is very large compared to the particle size: $D > 1.5$ μm. Since $h/D < 10^{-2}$, the right hand size term in equation (6) is always negligible and it can be assumed that the effective droplet volume fraction is equal to the actual oil volume fraction. In Figure 7, we observe that the normalized values of Π obtained for solid-stabilized emulsions all fall onto a single curve within reasonable experimental uncertainty. Our results were compared to the normalized data obtained by Mason et al. [6] in the presence of surfactants. These later are represented as a solid line which corresponds to the best fit to the experimental points. It is worth noting that the data for solid-stabilized emulsions are rather higher than the ones obtained in the presence of surfactants.

Another example illustrating the influence of the droplet size is given in Figure 9. The results correspond to dodecane-in-water emulsions which were all strongly aggregated (see Fig. 10). Again, we observe that the normalization by γ/R defines a unique plot that lies more than one decade above the curve corresponding to surfactant-stabilized emulsions. Therefore, it can be concluded that the osmotic resistance in solid-stabilized emulsions scales as $1/R$, at constant aggregation state and surface composition.

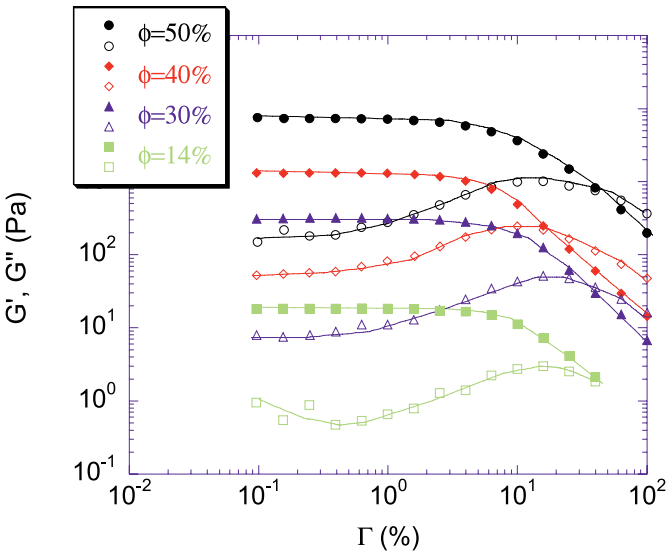

Fig. 11. Evolution of the rheological moduli G' and G'' with strain, Γ, at various droplets volume fractions. $D = 1.5$ μm.

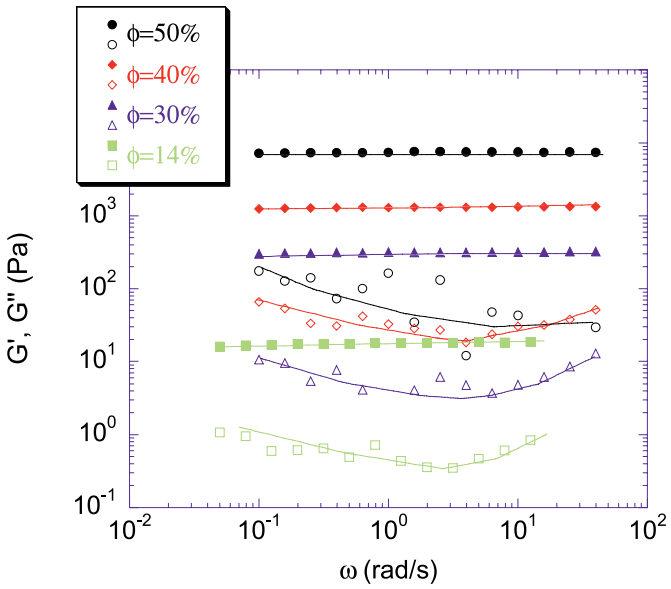

Fig. 12. Evolution of the rheological moduli G' and G'' with frequency, ω, at various droplets volume fractions. $D = 1.5$ μm.

2.2 Shear moduli

The rheological properties of emulsions can vary enormously; they can range from low viscosity fluids to highly elastic pastes. One interesting feature of solid-stabilized emulsions is that they behave like solids with high elastic moduli at relatively low droplet volume fractions ($\phi < \phi^*$). In this section, we measure the shear moduli of solid-stabilized emulsions, which should share many of the features described above for the osmotic resistance. Unfortunately, it was not possible to obtain G' and G'' for droplet fractions larger than 70% because of the unexpectedly high normal stresses exceeding the upper limit imposed by our rheometer. Although restricted to rather dilute emulsions, shear moduli measurements are useful since they provide a quantitative characterization of the elastic properties of the materials in a ϕ range that was not accessible to the osmotic resistance measurements ($\phi < 50\%$).

Typical results for both G' and G'' as a function of the applied oscillatory strain Γ, are shown in Figure 11 for several volume fractions of a strongly flocculated emulsion. The mother emulsion with mean droplet diameter $D = 1.5$ μm was fabricated at 10% and different samples at variable fractions ϕ were obtained by gentle centrifugation. For low strain values, G' is greater than G'' reflecting the essentially elastic nature of the materials. The significant level of elasticity below the random close packing is due to the tenuous network of interconnected droplets (see, e.g., Fig. 4b) that can bear stress. At large strains, there is a slight, gradual drop in the storage modulus, while the loss modulus begins to rise, indicating an approach to a non linear yielding behavior and plastic flow. At very large strains, beyond the yield stain marked by the drop in G', the apparent G'' dominates, reflecting the dominance of the energy loss due to non linear flow. The frequency dependence of the moduli is shown in Figure 12 for several values of ϕ and constant strain belonging to the linear regime. In all cases, there is a plateau in $G'(\omega)$ that extends over the full two decades of explored frequency. In contrast, for all ϕ, $G''(\omega)$ exhibits a shallow minimum. These results are reminiscent of those classically obtained for surfactant-stabilized emulsions [6].

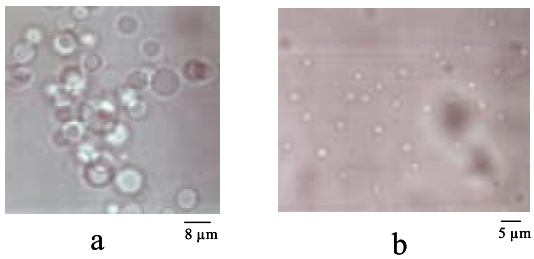

Fig. 13. Microscopic images of: a) PDMS-in-water emulsion with diameter $D = 8$ μm. b) The same emulsion sheared at $\tau = 3000$ Pa for 10 seconds.

2.3 Fragmentation experiments

Solid-stabilized PDMS droplets were dispersed in highly viscous solutions containing non adsorbing polymers (PEG or PAA). They were submitted to shear stresses of variable intensity following the protocol described in the experimental Section 1.2.6. We noticed that for both PEG and PAA solutions, droplet rupturing takes place above the same critical stress τ_c close to 3000 Pa. Below τ_c, the dispersed state remains invariant even if the stress is applied for several minutes while for $\tau > \tau_c$, droplet fragmentation is already accomplished after 10 seconds. In Figure 13, we show microscopic images of PDMS droplets dispersed in the PEG solution before (a) and after (b) application of a stress ($\tau = 3000$ Pa, for 10 s): the droplet

diameter is clearly smaller than the initial one, providing evidence that droplet fragmentation has occurred.

3 Discussion

3.1 Surface properties: elasticity and plasticity

The mechanical properties of concentrated emulsions are governed by their interfacial energy. Let us first consider interfaces at equilibrium. Any stress (osmotic or shear stress) imposed to the emulsion increases the amount of interface, leading to a modification of the free energy. For a monodisperse collection of N droplets of radius R, the total interfacial area of the undeformed droplets is $S_0 = 4\pi N R^2$. If the emulsion is compressed up to $\phi > \phi^*$, each droplet is pressing against its neighbors through flat facets. As a consequence, the total surface area, S, becomes larger than S_0. The osmotic resistance is thus the derivative of the free energy F with respect to the total volume V at constant number of droplets:

$$\Pi = -\left(\frac{\partial F}{\partial V}\right)_N = -\left(\frac{\partial F}{\partial S}\right)_N \left(\frac{\partial S}{\partial V}\right)_N. \quad (7)$$

The derivative of F with respect to S, $\sigma = \left(\frac{\partial F}{\partial S}\right)_N$, characterizes the mechanical behavior of the surface and is equal to the interfacial tension, γ, in the case of a surfactant-covered interface. A similar approach can be adopted for the bulk shear modulus. If the emulsion – already compressed to a surface S – experiences a small shear strain, Γ, the total interface increases quadratically with the strain – as shown by Princen [5]. The total droplet surface area increases thus as $S + \frac{1}{2}\Gamma^2 \left(\frac{\partial^2 S}{\partial \Gamma^2}\right)$. The bulk stress can be expressed as: $\tau = \frac{1}{V}\left(\frac{\partial F}{\partial \Gamma}\right)_N = \frac{\Gamma}{V}\left(\frac{\partial F}{\partial S}\right)_N \left(\frac{\partial^2 S}{\partial \Gamma^2}\right)$. The shear modulus is then given by:

$$G = \frac{1}{V}\left(\frac{\partial F}{\partial S}\right)_N \left(\frac{\partial^2 S}{\partial \Gamma^2}\right). \quad (8)$$

Hence, both the osmotic resistance and the bulk shear modulus can be expressed as products of two independent parameters, the derivative of the free energy with respect to the amount of interface and a geometrical factor $\left(\frac{\partial S}{\partial V}\right)_N$ and $\left(\frac{\partial^2 S}{\partial \Gamma^2}\right)$, representing the effect of a compression and of a strain respectively.

From the results of Mason et al. [6] it is easy to deduce the ϕ dependence of these two functions:

$$\left(\frac{\partial S}{\partial V}\right)_N = 1.7\frac{\phi^2(\phi^* - \phi)}{R} \quad (9)$$

and:

$$\left(\frac{\partial^2 S}{\partial \Gamma^2}\right) = 0.57 S_0 \phi(\phi - \phi^*). \quad (10)$$

It is worth noting that $\left(\frac{\partial S}{\partial V}\right)_N \approx -\frac{1}{V}\left(\frac{\partial^2 S}{\partial \Gamma^2}\right)$. This is a consequence of the fact that G and Π were found nearly equal for $\phi < 95\%$ in surfactant-stabilized emulsions [6]. Assuming that the factors $\left(\frac{\partial S}{\partial V}\right)_N$ and $\frac{1}{V}\left(\frac{\partial^2 S}{\partial \Gamma^2}\right)$ are purely geometrical and independent of the interface nature, following equations (7) and (8), we should identically obtain $G \approx \Pi$, in solid-stabilized emulsions.

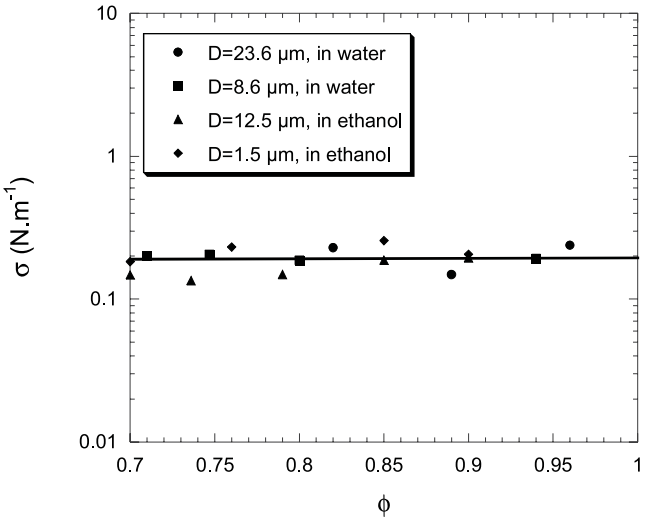

Fig. 14. Evolution of the surface modulus σ as a function of ϕ for emulsions comprising weakly aggregated PDMS droplets.

Since in solid-stabilized emulsions, the interfaces contain particles with attractive interactions, they are expected to behave like 2D solids. Let us first recall that the bulk elasticity originates mostly from the extension and the shear of the interfaces and not from their bending since the interfaces have a very small thickness, as compared to the radius of the droplets. More precisely, the ratio between the extensional energy and the buckling one – for instance swelling a shell from R to $R + \delta R$ – is about R^2/e^2 where e is the thickness of the interface (of the order of the particle diameter) which is negligible compared to R. Following equations (7) and (9), we can estimate the derivative of the free energy using the general relation:

$$\sigma = \left(\frac{\partial F}{\partial S}\right)_N = \frac{\Pi\ R}{1.7\phi^2(\phi - \phi^*)}. \quad (11)$$

Actually σ measures the bi-dimensional stress (also termed "tension") of the interface.

In Figure 14, we report the evolution of, σ as a function of ϕ for all the weakly flocculated emulsions comprising PDMS oil. In the explored ϕ range, we do not observe any variation of σ. This result reveals that the osmotic resistance in concentrated solid-stabilized emulsions can be described by a simple parameter, σ_0, independent of ϕ: in our case, $\sigma = \sigma_0 \approx 0.2\ \mathrm{N\,m^{-1}}$. In other words, the surface stress does not depend on the total amount of interface. On the one hand, the order of magnitude of σ_0 is not compatible with the interfacial tension, γ, measured between PDMS and water. On the other hand, this surface stress originates from the bi-dimensional network of the adsorbed solid particles that are known to exhibit strong lateral interactions. The fact that σ does not depend on

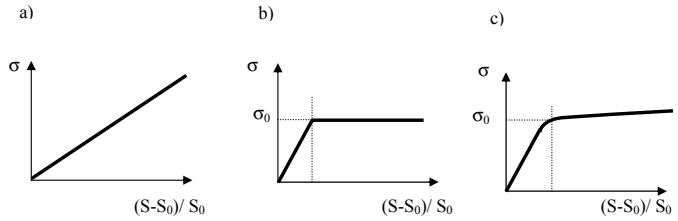

Fig. 15. Schematic mechanical behavior of the interface a) elastic behavior: the 2D stress is proportional to the relative surface extension, b) ideal plastic behavior: after a narrow elastic regime, the stress becomes constant and equal to σ_0 and c) standard plastic behavior: in the plastic regime, the stress slowly increases with the relative surface extension.

the surface area suggests that the surface stress saturates to a value which is probably the bi-dimensional yield stress for plasticity. In Figure 15, we schematically represent different possible mechanical behaviors of the interface. The abscissa represents the relative surface area extension, which is experimentally controlled by the droplet volume fraction ϕ, following equation (9). The purely elastic behavior in Figure 15a can be ruled out since it involves a strong variation of the surface stress σ with ϕ incompatible with the data of Figure 14. In contrast, an elastic regime followed by plastic behavior should result in either a constant stress, σ_0, for perfect plastic behavior, as sketched in Figure 15b, or a weak variation of σ for standard plastic behavior, as indicated in Figure 15c. The precision of our measurements does not allow distinguishing any variation in σ. Hence, at first order, we can be considered ideal plastic behavior characterized by a unique parameter σ_0. The elastic regime is certainly limited to very small deformations and is not accessible to our measurements. By integrating equation (9), we can calculate the relative surface excess:

$$\frac{S - S_0}{S_0} = \int_{S_0}^{S} \frac{dS}{S_0} = 0.3\,(\phi - \phi^*)^2\,. \qquad (12)$$

At $\phi = 70\%$ the relative surface excess is of the order of 0.1%. At this volume fraction, the surface stress has already reached its asymptotic value. Thus, the plastic strain of the surface is probably smaller than 0.1%.

For strongly flocculated emulsions, a large fraction of droplets is irreversibly bounded. Compaction of such "jammed" structures can only occur at the expense of deforming the droplet surfaces to a larger extend, revealed by the higher osmotic resistances measured experimentally. In Figure 16, we report the evolution of σ as defined by equation (11). We are aware that for such strongly flocculated structures, the variation of σ with ϕ does not merely represents the surface stress. Again, σ is independent of ϕ, but the constant σ_0 value ($\sim$1 N m^{-1}) that is obtained is only an apparent modulus that should be corrected by a factor 3−5 to account for the real properties of the surfaces.

The G values together with the osmotic resistance were normalized by σ_0/R and their variations with ϕ are

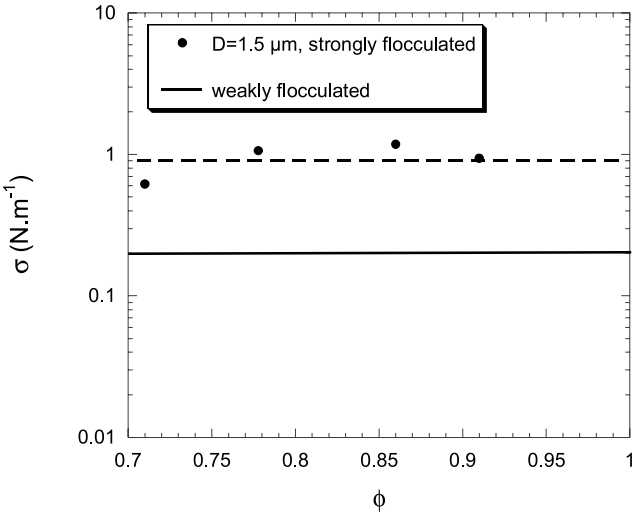

Fig. 16. Evolution of the surface modulus σ as a function of ϕ for emulsions comprising strongly aggregated PDMS droplets.

plotted in Figure 17. Figure 17a corresponds to strongly flocculated emulsions. As pointed above, neither Π nor G could be measured over the entire ϕ range but we managed to obtain both quantities at comparable ϕ values in a reduced number of systems. For those systems, the data obtained for G and Π were very close, again in agreement with the results obtained by Mason et al. for surfactant-stabilized emulsions [6]. Although the data are a little bit scattered, both series can reasonably be scaled onto a single master curve. For $\phi > \phi^*$, the data obey the following relation:

$$\Pi \approx G \approx 1.7\frac{\sigma_0}{R}\phi^2(\phi - \phi^*), \qquad (13)$$

in agreement with the previous discussion. The fact that $G \approx \Pi$ empirically confirms that $\left(\frac{\partial S}{\partial V}\right)_N \approx -\frac{1}{V}\left(\frac{\partial^2 S}{\partial \Gamma^2}\right)$ as in surfactant-stabilized emulsions.

Below ϕ^* and for strongly flocculated emulsions, Π and G are well described by:

$$\Pi \approx G \propto (\phi - \phi_0)^\alpha, \qquad (14)$$

ϕ_0 being close to zero and $\alpha \approx 4.5$. Comparable exponent values for the elastic modulus G have already been reported in dispersions of aggregated solid particles [12–14] or in jammed colloidal suspensions [15]. The σ_0 value fixes the magnitude of the shear modulus and is remarkably high ($\sim$1 N m^{-1}) for strongly flocculated emulsions. The data of Figure 17b were obtained with a weakly flocculated PDMS-in-water emulsion with mean diameter $D = 23.6$ μm. Again, the shear modulus, G, is rather elevated even below ϕ^* ($\phi > 50\%$) due to the intrinsic attractive interaction between the droplet surfaces mediated by solid particles. However, compared to Figure 17a, the normalized values are considerably smaller because of the much reduced density of irreversible bonds between the emulsion droplets (Fig. 8). For $\phi < \phi^*$, the behavior is very sensitive to the aggregated state; in principle, it should vary between the functional form given by equation (14) where ϕ_0 is very small (high irreversible bond density),

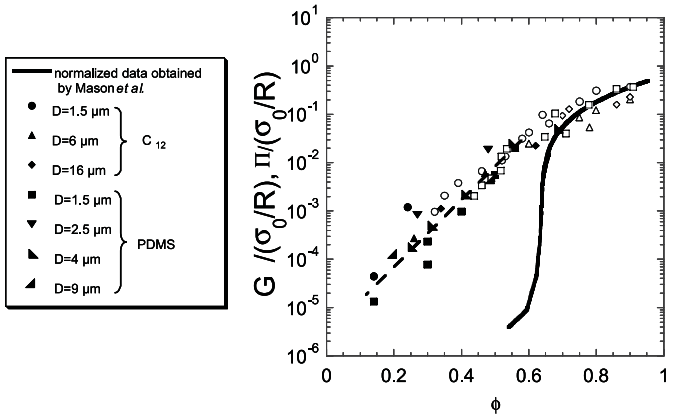

(a)

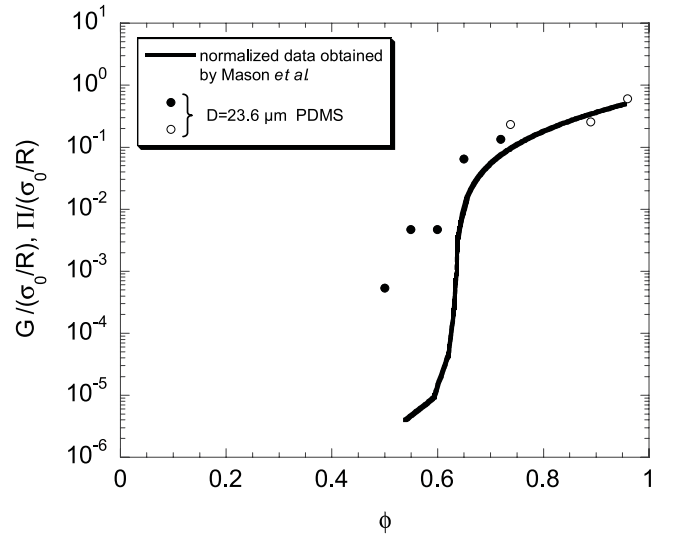

(b)

Fig. 17. Evolution of the shear modulus G (filled symbols) and the osmotic resistance Π (open symbols) for: a) strongly flocculated PDMS-in-water and dodecane-in-water emulsions of various sizes. The dashed line corresponds to the scaling: $G \propto \phi^{4.5}$. $\sigma_0 = 1\ \mathrm{N\,m^{-1}}$. b) weakly flocculated PDMS-in-water emulsion. $\sigma_0 = 0.2\ \mathrm{N\,m^{-1}}$. The solid line corresponds to the normalized data obtained by Mason et al. [6].

and almost zero (no measurable elasticity) for purely repulsive systems. Our weakly aggregated emulsions correspond to intermediate situations – ϕ_0 is of the order of 20%−30% – between the two previous limits. Note that this situation of weakly aggregated particles has also been described in [15] for solid suspensions. From our experiments, it seems that the bulk elasticity below ϕ^* mainly results from inter-drop connections and follows the classical behavior of adhesive suspensions, whereas above ϕ^* the bulk elasticity is dominated by the tension generated by 2-D plasticity.

3.2 Origin of σ_0. Influence of the inter-particle interactions

The droplet surface can be regarded as a compact 2-D network of solid particles with strong lateral attractive interactions. The surface stress tensor $\tilde{\sigma}$ is defined as $\tilde{\sigma} = \frac{\left\langle \vec{r} \otimes \vec{f} \right\rangle}{S}$ where $\otimes$ is the tensorial product, $\vec{r}$ and $\vec{f}$ are the position and force vectors respectively. At the onset of the plastic regime, surface clusters start to be dissociated and the yield stress σ_0 corresponds to the tangential component σ_{12}. If U is the pair potential of the adsorbed particles, then the yield stress can be estimated to be:

$$\sigma_0 \approx n_s \, \frac{z}{2} \left(\frac{d\,U}{d\,x} \right)_{x_0} x_0 \tag{15}$$

where x is the inter-particle distance, x_0 is the inter-particle distance at equilibrium (corresponding to a minimum for U), z is the coordination number ($z = 6$ for a 2-D hexagonal packing), n_s is the particle density at the interface. From $s_f = 24\ \mathrm{m^2\,g^{-1}}$, we deduce $n_s = 2.4 \times 10^{15}\ \mathrm{m^{-2}}$. The pair energy $e_a = x_0 \left(\frac{d\,U}{d\,x}\right)_{x_0}$ corresponding to the experimentally measured value $\sigma_0 = 0.2\ \mathrm{N\,m^{-1}}$ is then: $e_a \approx 7 \times 10^3\ kT$, kT being the thermal energy. In principle, three different types of interactions can contribute to the total attractive potential e_a: van der Waals forces, capillary forces, and the attractive interactions arising from the interpenetration of the octyl chains grafted on the solid particles. The van der Waals interaction energy between two identical spherical particles with diameter d_p is given by [16]:

$$e_{VdW} = \frac{A d_p}{12 x_0} \tag{16}$$

where A is the Hamaker constant ($A \approx 10^{-20}$ J for silica particles in water [16]). Assuming that x_0 is equal to the length of an extended octyl chain (0.6 nm), e_{VdW} can be evaluated to 4 kT. Capillary interactions arise from local deformations of the oil/water interface in the vicinity of the adsorbed particles [17,18]. Among the different types of capillary forces, at least one can generate attractive energies compatible with e_a. It originates from local deformations of the three phase contact line surrounding the particles [18]. If the line is not circular, but irregularly shaped with a characteristic deformation length l_c, the attractive potential between two particles at contact is given by:

$$e_c = \frac{3}{4} \pi \gamma l_c^2. \tag{17}$$

The functionalization process of the particles by octyl chains favors the formation of hydrophobic "patches" randomly distributed over the silica surfaces [19]. Therefore, the three phase contact line is certainly deformed at the scale of the characteristic size of the patches. Assuming that l_c is of the order of 20% of the particle circumference ($l_c \approx 0.2\pi d_p \approx 15$ nm), we find $e_c = 4 \times 10^3$ kT. Finally, a very strong interaction may arise from the interpenetration of the octyl layers [20]. Indeed, the octyl chains are in bad solvent in the continuous phase and consequently the layers tend to overlap:

$$e_o = \frac{2\pi d_p}{v_s} \phi_{ch} \left(L - \frac{x_0}{2} \right)^2 \left(\frac{1}{2} - \chi \right) \tag{18}$$

where v_s ($\approx 3 \times 10^{-30}$ m^3) is the molecular volume of the continuous phase, L($\approx$0.6 nm) is the extend of hydrophobic coating, ϕ_{ch} ($\approx$1) is the volume fraction of octyl chains in the brushes and χ ($\approx$8) is the Flory-Huggins interaction parameter. The resulting attractive interaction can vary between 0 ($x_0 > 2L$) to 3.5×10^4 kT ($x_0 = L$) depending on the interpenetration degree of the hydrophobic layers. It is likely that this type of interaction is also responsible for the aggregation of the solid particles in the water phase (prior to the emulsification), and of the oil drops once the emulsions are fabricated. The average octyltriethoxysilane chain density is rather high and overlapping of the hydrophobic layers is certainly an extremely slow process. This could explain why the aggregated state of either the particle suspensions or the solid-stabilized emulsions is sensitive to the mechanical treatment imposed to the samples during their preparation. A high energy stirring promotes partial or total dissociation of the interpenetrated layers which then take "infinite" time to overlap again.

The chemical nature of the continuous phase (water or ethanol) is expected to have an influence on the interparticle interactions. In the presence of ethanol, the emulsion droplets are rather dispersed, suggesting that ethanol is a better solvent for octyl chains than water and consequently the overlapping attraction is reduced. The impact of ethanol on capillary interactions is more difficult to predict but it is likely that this attraction increases owing to a more expanded conformation of the hydrophobic patches. The σ_0 value deduced from the Π versus ϕ plots for non flocculated systems is roughly the same for pure water and for pure ethanol. From empirical considerations, it can thus be concluded that the total attraction (capillary + chain overlapping) is not varying much from one solvent to the other.

To conclude this section, we believe that surface elasticity mainly results from capillary forces and from the interpenetration of the octyl layers in bad solvent. The magnitude of such interactions was evaluated and is of the same order than the total interaction energy deduced from σ_0.

3.3 Coalescence threshold

The very high value of the modulus σ_0 provides to emulsion films a strong resistance against coalescence. Film rupturing should imply the formation of large zones or fractures at the oil/water interface that are not covered by solid particles. It is clear that thermal fluctuations are unable to disrupt the very strong lateral links between the adsorbed particles and consequently, the spontaneous formation of large uncovered zones is completely inhibited. The only way to produce coalescence events consists of deforming the droplets to a sufficient degree so that their total surface area is extended. This may be achieved upon application of either a stress or an osmotic compression of the order of σ_0/R. To test this idea, different weakly aggregated PDMS-in-water (or PDMS-in-pure ethanol) emulsions were submitted to intense centrifugation fields corresponding to high osmotic resistances. Coalescence is revealed by the formation of a macroscopic oil layer that sits at the top (or bottom) of the samples and the main results are summarized in Table 1. By varying the droplet size, we observed that coalescence occurs above a unique value of the normalized osmotic resistance $\Pi^*/(\sigma_0/R) \approx 0.8$. This result suggests that film rupturing is associated to some critical relative deformation of the droplet surfaces, $\varepsilon_c = (S_c - S_0)/S_0$. The volume fractions at the onset of coalescence could not be measured with sufficient accuracy but we can state that they were always larger than 95%. Thus, a reasonable interval for ε_c is: $3\% < \varepsilon_c < 10\%$. The lower limit is provided by equation (12) at $\phi = 95\%$. The upper limit (10%) corresponds to the approximate relative deformation of a droplet adopting Kelvin's minimal tetrakaidecahedron shape at $\phi = 1$ [5].

Table 1. Critical osmotic resistance, Π^*, at the onset of coalescence for emulsions comprising PDMS drops.

continuous phase	D (μm)	Π^*(Pa)	$\Pi^*/(\sigma_0/R)$
water	8.6	36 000	0,8
	23.6	14 000	0,8
ethanol	1.5	163 500	0,8
	12.5	16 000	0,7

3.4 Shear experiments on single droplets

In this section, we propose a second route to measure the 2-D yield stress σ_0 based on the characteristic stress, τ_c, that produces droplet fragmentation (experimental Sect. 2.3). τ_c is expected to be of the order of the droplet deformability, i.e. σ_0/R, which allows an independent determination of σ_0.

The rupturing of an isolated droplet of one viscous fluid in another immiscible one is a classic problem in fluid mechanics with special relevance in the field of emulsification. The way in which the shear stresses induced by the flow overcome the interfacial tension between the two fluids to finally rupture the droplet has been addressed in increasing levels of detail since the pioneering work of Taylor [21]. Here, we report some of the main findings for the rupturing of a single droplet of viscosity η_d, suspended in a fluid having viscosity η_c, at low Reynold's number. The continuous phase is submitted to a shear stress τ. For rupturing to occur, the capillary number, $Ca = \tau R/\gamma$, defined as the ratio of the shear stress to the Laplace pressure, must exceed a critical value Ca_{cr}. This implies that the droplet has been elongated by the viscous shear before rupturing. A complete description of the deformation and bursting of isolated droplets under shear is complicated since the critical capillary number Ca_{cr} depends on the viscosity ratio η_d/η_c and the type and history of the shear flow [22–24] (see Fig. 18). Experiments have identified different rupturing scenarios that may occur when the shear

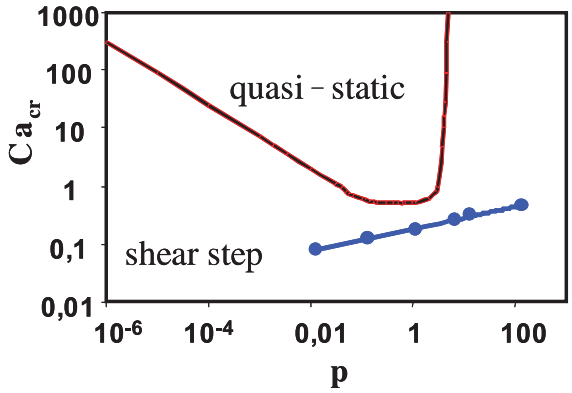

Fig. 18. Evolution of the critical capillary number, Ca_{cr}, as a function of the viscosity ratio p in both quasi-static [23] and non quasi-static [24] conditions. See text for details.

is increased very gradually (quasi-static conditions). Very recently, Mabille et al. [24] have explored the rupturing of isolated droplets in conditions where rapid transients in the shear rate are applied. Their experimental work focuses on fragmentation in simple shear flow conditions. Some of the main results can be summarized as follows:

(i) For $Ca > Ca_{cr}$, the droplet is stretched into elongated threads that undergo a capillary instability and breaks into a chain of many droplets. Such elongated droplet resembles a liquid cylinder that is susceptible to a capillary (Rayleigh) instability in which the surface tension drives the rupturing of the cylinder into many droplets having less total surface area.
(ii) The capillary instability takes place within a characteristic time smaller than 1 second.
(iii) The critical capillary number obeys the following empirical relation:

$$Ca_{cr} \approx 0.18\, p^{0.2}, \tag{19}$$

where $p = \eta_c/\eta_d$ is the viscosity ratio of the internal to the external phase (see Fig. 18).

Our method exploits the fact that the particles are irreversibly adsorbed and that there are no free particles in the continuous phase. The necessary condition for droplet rupturing to occur is that the initial droplets are deformed into long cylinders that undergo the Rayleigh instability. The particle concentration on the cylinders becomes considerably smaller than that on the initial undeformed droplets. It is likely that the surface behavior of the cylinders is dominated by interfacial tension, allowing the capillary instability to take place. However, according to the proposed model, the interface can be strongly deformed only if the applied stress exceeds the critical value σ_0. We therefore expect Ca_{cr} to be given by equation (19) with $Ca_{cr} = \tau_c R/\sigma_0$. We can now propose an estimation of σ_0 based on the critical stress for rupturing experimentally measured: $\tau_c \approx 3000$ Pa. The critical capillary number provided by equation (19) is $Ca_{cr} = 6.4 \times 10^{-2}$ for $p = 6 \times 10^{-3}$. We therefore obtain $\sigma_0 = \tau_c R/Ca_{cr} \approx 0.19\ \mathrm{N\,m^{-1}}$, in very good agreement with the value deduced from osmotic resistance measurements.

Conclusion

The experimental data reported in this paper provide indirect evidence for the existence of rigid interfacial layers in solid-stabilized emulsions. More precisely, a constant effective surface stress can account for the osmotic resistance, the elastic modulus, and the critical shear for rupturing of the droplets. This effective stress originates probably from the interactions between the colloidal particles within the interface.

Surface rigidity determines the remarkable resistance of concentrated droplets against coalescence. A recent paper reports that some solid-stabilized emulsions can even be dried without being destroyed until almost all the water is evaporated [11]. The original shape of the sample is preserved during the drying process, with absolutely no oil leakage, confirming the existence of a strong protective layer around the oil droplets. The resistance to coalescence is certainly determined by particle interactions as can be inferred from the general phenomenology established in the field of solid-stabilized emulsions: the most stable emulsions are very often obtained with solid particles that are weakly or strongly aggregated in the bulk continuous phase [4]. However, this correlation has to be handled with care since lateral interactions at the oil-water interface may be different from those in the continuous phase. More experimental and theoretical work is needed to consolidate (or refute) the validity of this empirical link. Finally, we should like to stress that some protein-stabilized emulsions obey the same phenomenology [25] (high osmotic resistances and shear moduli, strong resistance to water evaporation). Proteins possess the ability to form rigid interfacial aggregates [26,27] and it is likely that the description of the interface in terms of elasticity and plasticity can identically be applied to these systems.

This work was partially funded by Rhodia Services (France) and Le Conseil Régional d'Aquitaine. A. Omari is acknowledged for fruitful discussions and B.P. Binks for introducing the authors to solid-stabilized emulsions.

References

1. W. Ramsden, Proc. R. Soc. **72**, 156 (1903)
2. S.U. Pickering, J. Chem. Soc. **91**, 2001 (1907)
3. R.M. Wiley, J. Colloid Sci. **9**, 427 (1954)
4. B.P. Binks, Current Op. Colloid Interface Sci. **7**, 21 (2002)
5. H.M. Princen, Langmuir **2**, 519 (1986)
6. T.M. Mason, J. Bibette, D.A. Weitz, Phys. Rev. Lett. **75**, 2051 (1995)
7. M.-D. Lacasse, G.S. Grest, D. Levine, T.G. Mason, D.A. Weitz, Phys. Rev. Lett. **76**, 3448 (1996)
8. T.G. Mason, M.-D. Lacasse, G.S. Grest, D. Levine, J. Bibette, D.A. Weitz, Phys. Rev. E **56**, 3150 (1997)

9. T.H. Whitesides, D.S. Ross, J. Colloid Interface Sci. **169**, 48 (1995)
10. S. Arditty, C.P. Whitby, B.P. Binks, V. Schmitt, F. Leal-Calderon, Eur. Phys. J. E **11**, 273 (2003)
11. S. Arditty, J. Kahn-Giermanska, V. Schmitt, F. Leal-Calderon, J. Colloid Interface Sci. **275**, 659 (2004)
12. R.C. Ball, Physica D: Nonlinear Phenomena **38**, 13 (1989)
13. M.Y. Lin, H.M. Lindsay, D.A. Weitz, R.C. Ball, R. Klein, P. Meakin, Nature **339**, 360 (1989)
14. C.J. Rueb, C.F. Zubovski, J. Rheol. **41**, 197 (1997)
15. V. Trappe, V. Prasad, L. Cipelletti, P.N. Segre, D.A. Weitz, Nature **411**, 772 (2001)
16. J.N. Israelachvili, *Intermolecular and surface forces* (New York, 1992)
17. P.A. Kralchevsky, K. Nagayama, Adv. Colloid Interface Sci. **85**, 145 (2000)
18. P.A. Kralchevsky, N.D. Denkov, Current Op. Colloid Interface Sci. **6**, 383 (2001)
19. S. Arditty, Ph.D. thesis, Bordeaux 1, 2004
20. S.R. Raghavan, J. Hou, G.L. Baker, S.A. Kahn, Langmuir **16**, 1066 (2000)
21. G.I. Taylor, Proc. R. Soc. A **146**, 501 (1934)
22. J.M. Rallison, Annu. Rev. Fluid Mech. **16**, 45 (1984)
23. H.P. Grace, Chem. Eng. Commun **14**, 225 (1982)
24. C. Mabille, F. Leal-Calderon, J. Bibette, V. Schmitt, Europhys. Lett. **61**, 708 (2003)
25. T.D. Dimitrova, F. Leal Calderon, Langmuir **17**, 3244 (2001)
26. T.D. Dimitrova, F. Leal Calderon, Adv. Colloid Interface Sci. **108**, (2004)
27. L. Bressy, P. Hébraud, V. Schmitt, J. Bibette, Langmuir **19**, 598 (2003)